JOC*Article*

Intramolecular General Acid Catalysis of the Hydrolysis of 2-(2′-Imidazolium)phenyl Phosphate, and Bond Length−Reactivity Correlations for Reactions of Phosphate Monoester Monoanions

Tiago A. S. Brandão,[†] Elisa S. Orth,[†] Willian R. Rocha,[‡] Adailton J. Bortoluzzi,[†] Clifford A. Bunton,[§] and Faruk Nome*[,†]

Departamento de Química, Universidade Federal de Santa Catarina, Florianópolis, SC 88040-900, Brazil, Departamento de Química, ICEX, Universidade Federal de Minas Gerais, Belo Horizonte, Minas Gerais, 31270-901, Brazil, and Department of Chemistry and Biochemistry, University of California, Santa Barbara, California 93106-9510

faruk@qmc.ufsc.br

Received January 16, 2007

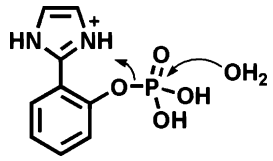

Rate constants for the hydrolysis of 2-(2′-imidazolium)phenyl hydrogen phosphate (IMPP) in water at pH < 6 indicate that activation by the imidazolium moiety disappears with the deprotonation of the phosphate group, and the reaction involves the hydrogen-bonding of the imidazolium NH with the aryl oxygen leaving group. The reaction should involve a near-planar conformation of the imidazolium and the phenyl groups in the activated complex, which favors proton-transfer. The crystal structure of IMPP was solved, and a bond length−reactivity correlation for reactions of phosphate monoester monoanions is described.

Introduction

General acid catalysis plays a central role in many biological processes, such as the phosphoryl transfers of phosphate monoester or the cleavage of diesters (e.g., of RNA and DNA), where, in the absence of a catalytic metal, proton activation assists P−O bond breaking. General acid−base catalysis has been shown to be important in some simple models for phosphate transfer reactions,[1,2] and the common feature of these efficient intramolecular model systems is a strong intramolecular hydrogen-bond in both the product and the activated complex. Phosphorylation of a variety of nucleophiles by the 8-dimethylammonium-naphthyl-1-phosphate monoanion is effectively general acid catalyzed by the neighboring NH^+ group, by a factor of ca. 10^6. Similar catalytic effects due to strong intramolecular hydrogen-bonding have been demonstrated in sulfuryl transfers of 8-dimethylammonium-naphth-1-ol derivatives, **1**, to water or other nucleophiles with rate increases of 10^6-10^8 fold.[1,2]

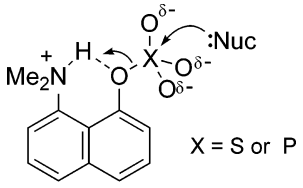

1

Although useful, models can be speculative because the quantitative analysis is usually difficult and is limited by a lack of structural data (e.g., crystallographic) that would help to clarify the role of proton-transfer or other specific mechanistic effects. In practice, the accelerations of sulfuryl and phosphoryl transfers that are caused by the introduction of the dimethylammonium group in **1** are related, at least in part, to the significant hydrogen-bonding in the reactant monoesters; unfortunately, crystallographic data are not available. Here, we show the newly solved structure of 2-(2′-imidazolium)phenyl

* To whom correspondence should be addressed. Telephone: +55-48-37216849, fax: +55-48-37216850.
[†] Universidade Federal de Santa Catarina.
[‡] Universidade Federal de Minas Gerais.
[§] University of California.

(1) Kirby, A. J.; Dutta-Roy, N.; Silva, D.; Goodman, J. M.; Lima, M. F.; Roussev, C. D.; Nome, F. *J. Am. Chem. Soc.* **2005**, *127*, 7033−7040.
(2) Kirby, A. J.; Gesser, J. C.; Hollfelder, F.; Priebe, J. P.; Nome, F. *Can. J. Chem.* **2005**, *83*, 1629−1636.

10.1021/jo070090r CCC: $37.00
Published on Web 04/14/2007

hydrogen phosphate (IMPP) and crystallographic results that indicate a clear structure−reactivity relationship[3] in the reactions of phosphate monoester monoanions. We also have evaluated the intramolecular proton-transfer efficiency in the hydrolysis of IMPP over a range of H_0 −4.2 to pH 6.

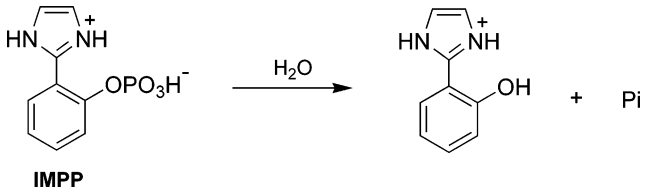

IMPP

Results and Discussion

Titration Studies. Acid dissociation constants of IMPP were determined potentiometrically in the pH range 2−9; two pK_a values were found: 4.67 ± 0.02 and 7.47 ± 0.04. A spectrophotometric titration method was used to assign these values to hydroxyl and imidazolium groups and to confirm the pK_a values. Spectral scans were performed from pH 2.0−9.0 at 295 nm and resulted in pK_a values of 4.78 ± 0.14 and 7.49 ± 0.05 (Figure 1). We observed a smaller change in absorbance for the first pK_a as compared to the second. This suggests that the second pK_a corresponds to the deprotonation of an imidazolium nitrogen, which in turn affects conjugation with the phenyl group. These results are confirmed by ^{31}P NMR titration measurements. The ^{31}P signal (Figure 1b) shows a large upfield shift between pH 4.5 to 6.5 but shows a small change above pH 7, which is consistent with −POH and then −NH deprotonation.

Scheme 1 is consistent with the titration studies. IMPP is written as a zwitterion, IMPP$^{\pm}$, with the imidazolium group written as a classical structure. Protonation of IMPP$^{\pm}$ forms IMPP^{+} (the pK_a = −1.17 was kinetically determined, vide infra). With increasing pH, deprotonation generates IMPP^{-} and IMPP^{2-} with the pK_a values reported above.

Kinetics. The hydrolysis of IMPP was followed as a function of acidity in the range of H_0 −4.2 to pH 6 (Figure 2). Acid catalysis in the H_0 region[4,5] indicates that IMPP$^{\pm}$ is protonated in higher HCl concentrations to form reactive IMPP^{+}. The hydrolysis rate maximum at $H_0 \approx -2$ (HCl ∼6 M) is both qualitatively similar to those observed for many aryl and naphthyl phosphate esters with strongly electron-withdrawing substituents[1,6−8] and is typical of hydrolysis reactions that involve the attack of a water molecule in the rate-limiting step.[7]

In Figure 2, the open squares are for a plot of log k_{obs} against Hammett's acidity function, H_0 (= −log h_0). The solid squares include a first-order correction for water activity (k_{obs}/a_w) at 60 °C, with extrapolation of the Åkerlöf and Teare data in the range of 0−50 °C.[9] The values of the rate constants, both the uncorrected and those with the first-order correction (k_{obs}/a_w), go through maxima, which indicates that the order of the reaction with respect to water may be higher than one or that the extent of hydration changes. More than one water molecule appears to be involved in these reactions, but the activity effects on the substrate are not explicitly considered. A similar high dependence on water activity is indicated by Bunnett's *w* and φ values (eqs 1 and 2). The values are derived from the slopes of the plots of log k_{obs} + H_0 against log a_w (eq 1) or H_0 + log[HCl] (eq 2), respectively.[10,11]

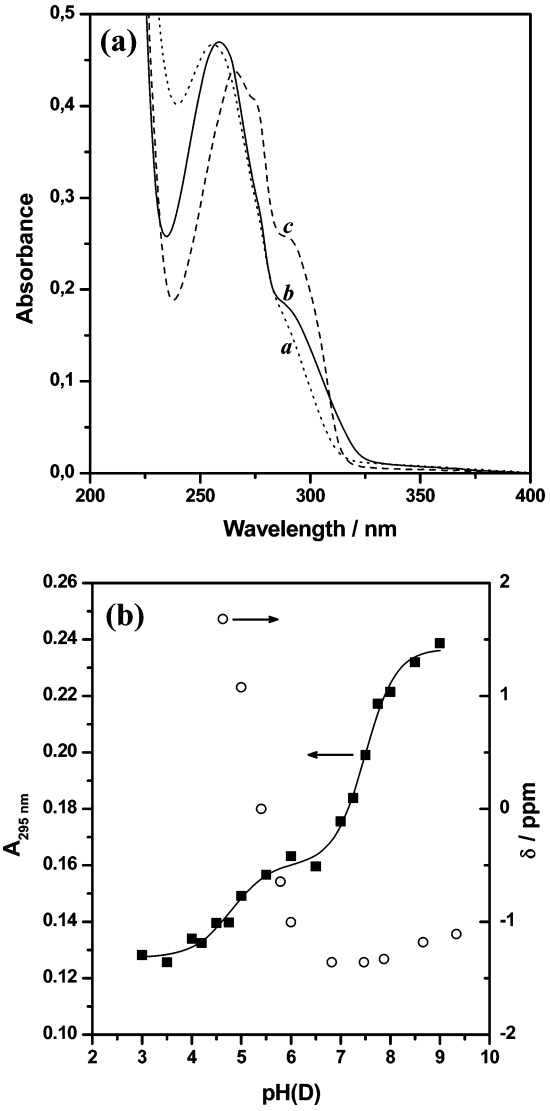

FIGURE 1. (a) Spectrophotometric scans of aqueous 66.7 μM IMPP at pH 3.0 (*a*), 6.0 (*b*) and 9.0 (*c*); (b) Absorbance at 295 nm (■) and ^{31}P NMR shifts (○) as functions of pH and pD, respectively, at 25.0 °C. The extinction coefficients at 295 nm of the zwitterion, the monoanion, and the dianion of IMPP are 1904, 2607, and 3553 $M^{-1}\cdot cm^{-1}$, respectively.

SCHEME 1

$$IMPP^{+} \overset{pK_a = -1.17}{\rightleftharpoons} IMPP^{\pm} \overset{pK_a = 4.67}{\rightleftharpoons} IMPP^{-} \overset{pK_a = 7.47}{\rightleftharpoons} IMPP^{2-}$$

$$\log k_{obs} + H_0 = w \log a_w + \text{constant} \quad (1)$$

$$\log k_{obs} + H_0 = \varphi(H_0 + \log[HCl]) + \text{constant} \quad (2)$$

These Bunnett parameters (*w* and φ) were originally applied to the hydrolysis of esters that are nonionic or are present as

(3) Kirby, A. J. *Adv. Phys. Org. Chem.* **1994**, *29*, 87−183.
(4) (a) Anslyn, E. V.; Dougherty, D. A. *Modern Physical Organic Chemistry*; University Science Books: Sausalito, CA, 2006. (b) Lowry, T. H.; Richardson, K. S. *Mechanism and Theory in Organic Chemistry*; Harper & Row: New York, 1987.
(5) Paul, M. A.; Long, F. A. *Chem. Rev.* **1956**, *56*, 1−45.
(6) Bunton, C. A.; Fendler, E. J.; Humeres, E.; Yang, K.-U. *J. Am. Chem. Soc.* **1967**, *32*, 2806−2811.
(7) Bunton, C. A.; Fendler, E. J.; Fendler, J. H. *J. Am. Chem. Soc.* **1967**, *89*, 1221−1230.
(8) Bunton, C. A.; Farber, S. J. *J. Org. Chem.* **1969**, *34*, 767−772.
(9) Åkerlöf, G.; Teare, J. W. *J. Am. Chem. Soc.* **1937**, *59*, 1855−1869.

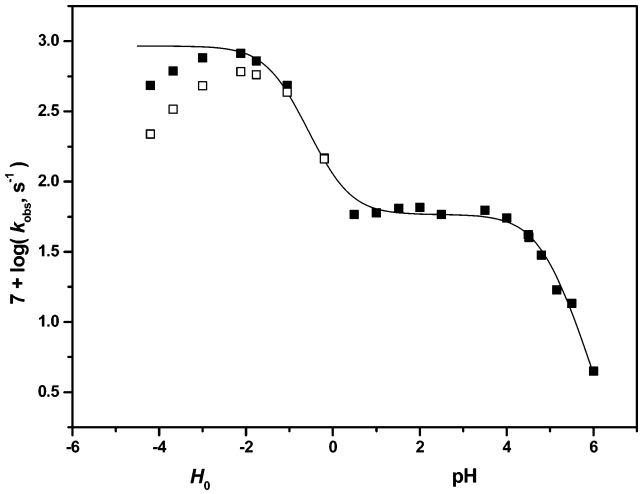

FIGURE 2. Plot of log k_{obs} against pH or H_0 (pH < 0) for the hydrolysis of IMPP at 60.0 °C. Kinetic data with (■) and without (□) the correction for water activity. The line is theoretical (eq 3), with the parameters shown in Table 2. The H_0 values at 25 °C are from Paul and Long.[5]

phosphoric acids, and the Hammett acidity function, H_0, was estimated for the protonation of nonionic bases, which limits the quantitative application of eq 1 and eq 2. We estimated $w = 11.6$ ($n = 7$, $R = 0.998$) and $\varphi = 1.31$ ($n = 7$, $R = 0.998$) for the acid hydrolysis of $IMPP^+$. These values are similar to the values $w = 10.9$ ($n = 12$, $R = 0.997$) and $\varphi = 1.18$ ($n = 12$, $R = 0.996$) that were calculated from data[1] for the acid hydrolyses of the structurally related **1**. They are also similar to values for the hydrolysis of other aryl phosphate esters in hydrochloric, sulfuric, and perchloric acids,[8] where values of $w = \sim 7$ and $\varphi = \sim 1.2$ were reported, and it was suggested that the hydrolysis process involves a slow proton-transfer, which could be concerted with the attack of water and the strong hydration of the acidic hydroxyl groups of the phosphate moiety in the activated complex.[10]

The meaning of order with respect to water in solvolytic reactions is a very uncertain concept. However, a nucleophilic attack by water usually involves two water molecules, with proton-transfer from one to the other. In the reactions of $IMPP^+$ and $IMPP^{\pm}$, one water molecule forms a new bond with phosphorus, but other water molecules are involved in hydrogen-bonding or proton-transfer or interact with polar or ionic centers to differing extents as the reaction progresses. However, the parameters in eqs 1 and 2 indicate the sensitivity of the reaction to the availability of water.

TABLE 1. Acid Dissociation Constants at 25.0 °C and Kinetic Parameters for Hydrolysis of IMPP at 60.0 °C

constant	value
$pK_a(1)$	-1.17 ± 0.16^a
$pK_a(2)$	4.67 ± 0.02^b
$pK_a(3)$	7.47 ± 0.04
k_1, s^{-1}	$(8.67 \pm 0.57) \times 10^{-5}$
k_2, s^{-1}	$(5.83 \pm 0.18) \times 10^{-6}$

[a] The pK_a was calculated from kinetic data in HCl in the H_0 region (see text) at 60.0 °C [b] $pK_a = 4.90 \pm 0.36$ at 60.0 °C.

At pH 0−6, the rate profile is similar to those observed for phosphate monoesters with a leaving group $pK_a > 5.5$,[12] and the reaction of the zwitterion (i.e., $IMPP^{\pm}$) is much faster than spontaneous reactions of the mono- and dianions. Scheme 2 accords with the experimental results and is consistent with eq 3. In the H_0−pH range studied, only reactions of cations and zwitterions are considered. The rate and equilibrium constants from a least-squares fit are in Table 1. Including the contribution of the monoanion, $IMPP^-$, does not significantly affect the constants. The pK_{a1} value based on H_0 is reasonable but is also uncertain. However, the values for similar phosphate esters are ca. −1.5.[1,13] The pK_{a2} value of 4.90 ± 0.36 at 60 °C is consistent with the kinetic evidence. Protonation in the H_0 range is at acidities where the pH scale is not applicable, as is typical with the hydrolysis of other aryl phosphates. Scheme 2 illustrates the overall reactions involved in the different hydrolyses, although we do not explicitly include the concentration or activity of water.

$$k_{obs} = k_1\left(\frac{[H^+]h_0}{[H^+]h_0 + K_{a1}[H^+] + K_{a1}K_{a2}}\right) + k_2\left(\frac{K_{a1}[H^+]}{[H^+]h_0 + K_{a1}[H^+] + K_{a1}K_{a2}}\right) \quad (3)$$

$IMPP^+$ Hydrolysis. The hydrolysis of the cationic species, $IMPP^+$ (as the phosphoric acid derivative), is much faster than those of dialkyl aryl phosphates,[14] and the estimated rate enhancement for the hydrolysis of $IMPP^+$, as compared with a triester derived from a phenol of pK_a 10, is about 10^6 at 60 °C.[7,14] This effect is not unprecedented. For the acid hydrolysis of 8-dimethylammonium-naphthyl-1-phosphoric acid, a rate enhancement of ca. 10^8 was reported, and in both reactions there is little or no hydrogen-bonding stabilization when the phosphate group is neutral.[1] The reaction of $IMPP^+$ is slower than that of the dihydrogen phosphate that is derived from 8-dimethylami-

SCHEME 2

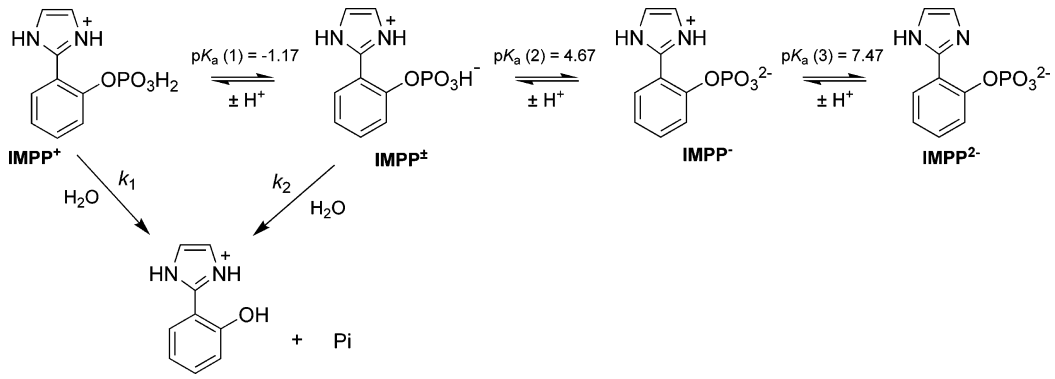

SCHEME 3

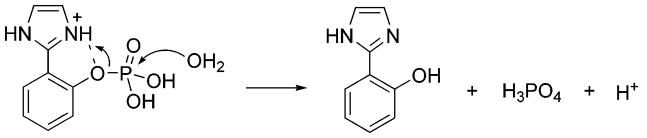

nonaphth-1-yl.[1] In the rigid naphthyl derivative, **1**, the effective molarity of the transferring proton is higher than in IMPP$^+$, where proton-transfer to the bridge oxygen involves the loss of degrees of rotational freedom of the imidazolium group.

The reaction in the acidic region is shown in Scheme 3, where protonation of the anionic phosphate generates IMPP$^+$, and a water molecule attacks the phosphorus phosphoric acid center while proton-transfer from the imidazolium moiety to the aryl oxygen atom strongly favors P−O cleavage. Proton-transfer to the bridging oxygen may involve hydrogen-bonding, and its extent would increase as the reaction progresses. In the initial state, there will be hydrogen-bonding of the imidazolium NH to water and also to the bridging and phosphoryl oxygens. As the reaction progresses, the hydrogen-bonding to water should decrease and that to the bridging oxygen will increase, and at the end of the reaction, this proton-transfer should be complete.

As in the hydrolysis of the naphthyl derivative, **1**, the hydrolysis of IMPP$^+$ does not appear to involve a stepwise mechanism, with pre-equilibrium proton-transfer from protonated nitrogen to the bridge oxygen. In both cases, the pK_a of the conjugate acid of the bridge oxygen is much lower than that of the general acid (either imidazolium in IMPP$^+$ or dimethyl ammonium in **1**). Proton-transfer from the imidazolium group with increasing strength of the hydrogen-bond should be concerted with the phosphorylation of water, which would generate a negative charge on the bridge oxygen, unless it is neutralized by intramolecular protonation in the course of the reaction.

IMPP$^\pm$ Hydrolysis. In principle, two different activation roles for the imidazolium moiety can be envisioned in the hydrolysis of IMPP$^\pm$, viz. hydrogen-bonding between N−H and the bridge oxygen (**2**), which should assist P−O bond cleavage, or with the nonbridged phosphoryl oxygen (**3**), which should assist the attack of water on phosphorus.

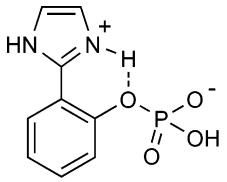

2

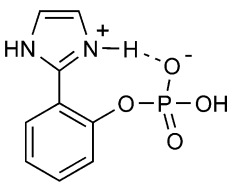

3

Both catalytic roles have been considered in phosphate ester hydrolyses. The first is highly effective, and accelerations are typically greater than 10^6 fold.[1,15] The other is less effective.

TABLE 2. Selected Bond Lengths (Å) and Angles (°) for IMPP and HPI[17]

compound	IMPP	HPI
C1−N5	1.326(4)	1.327(2)
C1−N2	1.336(3)	1.353(2)
C1−C11	1.470(4)	1.450(2)
C12−O1	1.379(3)	1.363(2)
P1−O4	1.478(2)	
P1−O3	1.499(2)	
P1−O2	1.560(2)	
P1−O1	1.626(2)	
N5−C1−N2	107.2(2)	109.8(2)
N5−C1−C11	128.5(2)	124.3(2)
N2−C1−C11	124.0(2)	125.9(1)
C1−N2−C3	109.6(2)	107.8(2)
C1−N5−C4	109.3(2)	106.3(2)
O1−C12−C13	123.3(3)	119.1(2)
O1−C12−C11	117.2(2)	120.3(2)
C12−O1−P1	124.9(2)	
N5−C1−C11−C12	38.6(3)	−1.2(3)
C1−C11−C12−O1	6.5(4)	0.8(3)

IMPP	D−H	H···**A**	D···**A**	D−H···**A**
N2−H2···O3[a]	0.83	1.85	2.673(3)	168.4
N5−H5···O4[b]	1.03	1.62	2.618(3)	163.3
2-(2′-hydroxyphenyl)imidazole				
O1−H1···N5	1.13	1.48	2.545(2)	154.3

[a] Symmetry code: $y, -x + y + 1, z + 1/6$. [b] Symmetry code: $y, -x + y, z + 1/6$.

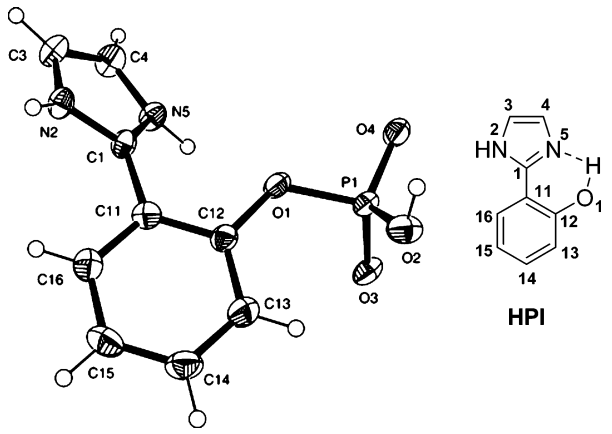

FIGURE 3. Molecular structure of IMPP, showing ellipsoids at the 40% probability level. Hydrogens are numbered according to the heavy atoms.

For example, Anslyn et al.[16] observed that guanidinium activation in phosphate diester cleavage can provide only a 40-fold rate enhancement. The source of this large difference is probably related to the freedom of rotation in the phosphoryl moiety and the strength of the hydrogen-bonding. To improve our understanding of the latter effect, we examined the crystal structure of IMPP$^\pm$. In these reactions of **1** and IMPP, the neighboring ammonium or imidazolium NH, as a hydrogen donor, displaces the water molecule(s) that initially solvate the bridging oxygen.

X-ray Crystallography. Table 2 summarizes selected bond lengths and angles of IMPP$^\pm$ with the atom-numbering in Figure 3. For comparison, the geometry of 2-(2′-hydroxyphenyl)-imidazole (HPI) is known from X-ray diffraction.[17]

There are several significant structural differences between IMPP$^\pm$ and its counterpart, HPI, and the most important are

(10) Bunnett, J. F. *J. Am. Chem. Soc.* **1961**, *83*, 4956−4967, 4968−4973, 4973−4977, 4978−4983.
(11) Bunnett, J. F.; Olsen, F. P. *Can. J. Chem.* **1966**, *44*, 1899−1916, 1917−1931.
(12) Kirby, A. J.; Varvoglis, A. G. *J. Am. Chem. Soc.* **1967**, *89*, 415−423.
(13) Kirby, A. J.; Lima, M. F.; Silva, D.; Roussev, C. D.; Nome, F. *J. Am. Chem. Soc.* **2006**, *128*, 16944−16952.
(14) Khan, S. A.; Kirby, A. J. *J. Chem. Soc. B* **1970**, 1172−1182.
(15) Bromilow, R. H.; Kirby, A. J. *J. Chem. Soc., Perkin Trans.* **1972**, *2*, 149−155.
(16) Piatek, A. M.; Gray, M.; Anslyn, E. V. *J. Am. Chem. Soc.* **2004**, *126*, 9879−9879.

(i) the C1−C11 bond is longer by 0.020 Å in IMPP$^{\pm}$ than in HPI because the imidazole and phenyl groups have a resonance interaction that is reduced by rotation about the C1−C11 bond in IMPP$^{\pm}$; (ii) in HPI, the C1−N5 and C1−N2 bonds are as expected for a simple nonionic imidazole,[18] with one bond longer than the other by 0.025 Å. For IMPP$^{\pm}$, the situation reflects that of a protonated imidazole,[19] where the C−N bond lengths are very similar with a difference of only 0.003 Å. However, the C1−N5 and the C1−N2 bond lengths differ by 0.010 Å in IMPP$^{\pm}$ (Table 2), which is an indication of the H5 hydrogen-bonding with O4 of an adjacent molecule of IMPP$^{\pm}$ in the crystal. The separation of H5 from O4 of a neighboring molecule is only 1.618 Å.

The geometry of the activated complex for hydrolysis of IMPP$^{\pm}$ is governed by the proton-transfer to the bridged oxygen, O1. Distances between the imidazolium nitrogen N5 and the aryl oxygen O1 are 2.9 Å in IMPP$^{\pm}$ and 2.5 Å in the derivative, phenol HPI, and are typical of low barrier hydrogen-bonds.[17] Thus, it appears that rotation about the C1−C11 bond in IMPP allows for the formation of the activated complex, and attack of the water molecule is concerted with the proton-transfer to O1 as shown in **3**. The molecular geometry in the crystal is probably not that found in water, but the conformation in the solid is indicative of a weaker hydrogen-bond than in HPI, which indicates that in aqueous solution intramolecular hydrogen-bonding is probably not important in the initial state but strengthens in the course of the reaction.

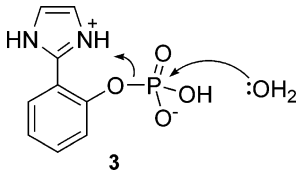

3

The pK_a of the conjugated acid of the leaving group is lower than that of a simple aryl hydrogen phosphate, which is derived from a phenol of pK_a 10, and a survey of structures in the Cambridge Structural Database (CSD) supports this conclusion. Indeed, there is a linear relationship between the pK_a of the conjugate acid of the leaving group (pK_{LG}) and the C−O bond length, and the longest C−O bond corresponds to the shortest P−O bond, with the sum of the two bond lengths effectively constant at 3.014 Å (Figure 4; see details in Supporting Information).

The slope of -5.5×10^{-3} units ($R = 0.929$) for the P−O bond length correlation with pK_{LG} (Figure 4) is consistent with results on the corresponding correlations for phosphate monoester dianions,[21] RO−PO_3^{2-}, and sulfate ester monoanions,[22] RO−SO_3^-, with slopes of -8×10^{-3} and -5.3×10^{-3}, respectively. The P−O bond lengths of the phosphate monoester monoanions are less sensitive to the basicity of the leaving group than for phosphate monoester dianions but are similar to those for sulfate ester monoanions. This observation agrees with the suggested effective charge on the leaving oxygen of the initial states, which is +0.7 for the sulfate, +0.36 for the phosphate monoester dianions, but +0.74 for the monoanions.[23]

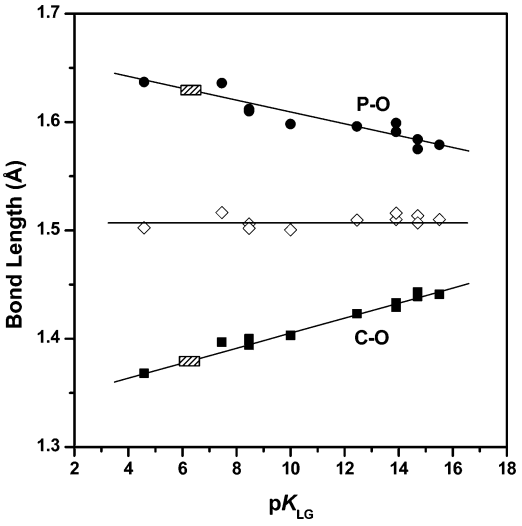

FIGURE 4. Dependence of C−O and P−O_{bridge} bond lengths on pK_{LG} in phosphate monoester monoanions.[20] The constant sum of the two bond lengths is shown by the zero slope of the middle line, which is a plot of $(l_{C-O} + l_{P-O})/2$. Hatched regions correspond to the bond lengths of IMPP within a possible range for pK_{LG}, see the text for details.

The pK_{LG} for IMPP$^{\pm}$ from P−O and C−O bond lengths is approximately 6.5 (Figure 4), which is a direct consequence of intramolecular hydrogen-bonding between H5 with O1 and H2 with O1 of an adjacent molecule in the crystal, with distances of 2.683 and 2.735 Å, respectively. Thus, in going from the initial state to the activated complex, the bridge oxygen atom O1 could accept the proton H5 of the imidazolium group, which rotates about the C1−C11 bond to become approximately coplanar with the phenyl ring. P−O bond cleavage, which dominates the formation of the activated complex, is favored by this coplanarity. Coplanarity also favors the developing negative charge on the aryloxy leaving group by promoting delocalization with the imidazolium group and by favoring hydrogen-bond proton-transfer from the imidazolium H5 (Figure 3).

It is interesting that the proton inventory at pH 3.00 was a straight line with no apparent kinetic solvent isotope effect (KSIE, $k_{H_2O}/k_{D_2O} = 1.00 \pm 0.06$). For compounds such as IMPP$^{\pm}$ and **1**, measurements of KSIE are not very useful because they are generally small. In the present case, as was suggested by a reviewer, a nonlinear proton-transfer (e.g., by increasing hydrogen-bond strength) with a change in binding force constants should lead to a small deuterium isotope effect. For linear proton-transfers, solvent hydrogen isotope effects should be small if, in the activated complex, there is either little

(17) Foces-Foces, C.; Llamas-Saiz, A. L.; Claramunt, R. M.; Cabildo, P.; Elguero, J. *J. Mol. Struct.* **1998**, *400*, 193−202.

(18) McMullan, R. K.; Epstein, J.; Ruble, J. R.; Craven, B. M. *Acta Crystallogr.* **1979**, *B35*, 688−691.

(19) Fukunaga, T.; Ishida, H. *Acta Crystallogr.* **2003**, *E59*, o1869−o1871.

(20) (a) Weichsel, A.; Lis, T. *Acta Crystallogr.* **1992**, *C48*, 303−305. (b) Cherepinskii-Malov, V. D.; Struchkov, Y. T.; Gurarii, L. I.; Mukmenev, E. T.; Arbuzov, B. A. *Zh. Obshch. Khim. (Russ.) (Russ. J. Gen. Chem.)* **1985**, *55*, 2457−2461. (c) Weber, H. P.; Petcher, T. J. *J. Chem. Soc., Perkin Trans.* **1974**, *2*, 942−946. (d) Glowiak, T.; Szemik, A. W. *J. Crystallogr. Spectrosc. Res.* **1986**, *16*, 79−89. (e) Lis, T. *Carbohydr. Res.* **1992**, *229*, 33−39; Kraut, J. *Acta Crystallogr.* **1961**, *14*, 1146−1152. (f) Weber, H.-P.; McMullan, R. K.; Swaminathan, S.; Craven, B. M. *Acta Crystallogr.* **1984**, *B40*, 506−511. (g) Lis, T. *Carbohydr. Res.* **1985**, *135*, 187−194. (h) Narendra, N.; Viswamitra, M. A. *Acta Crystallogr.* **1985**, *C41*, 1621−1624. (i) Kerr, K. A.; Fawcett, J. K.; Coppola, J. C.; Watson, D. G.; Kennard, O. *Acta Crystallogr.* **1979**, *B35*, 2749−2751.

(21) Jones, P. G.; Kirby, A. J. *J. Am. Chem. Soc.* **1984**, *106*, 6207−6212.

(22) Brandão, T. A. S.; Priebe, J. P.; Damasceno, A. S.; Bortoluzzi, A. J.; Kirby, A. J.; Nome, F. *J. Mol. Struct.* **2005**, *734*, 205−209.

(23) Williams, A. *Free Energy Relationships in Organic and Bio-organic Chemistry*; RSC: Cambridge, 2003.

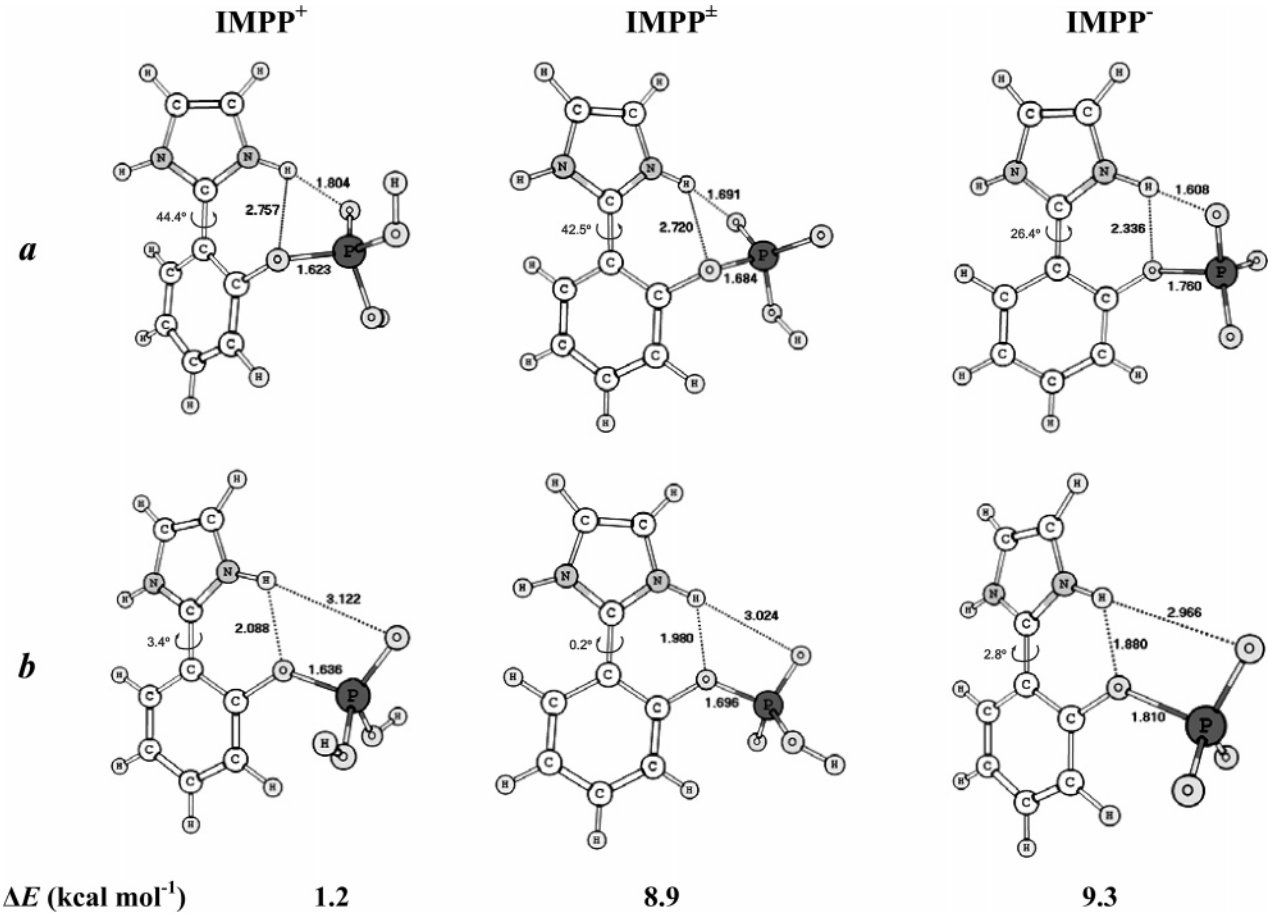

FIGURE 5. B3LYP optimized structures of $IMPP^+$, $IMPP^{\pm}$ and $IMPP^-$ and relative energies ΔE ($E_b - E_a$) describing the preference between conformers with hydrogen-bonding, NH···O4 (**a**) and NH···O1 (**b**). The bond lengths and distances are given in Å, and dihedral angles are in degrees.

or extensive proton-transfer. The situation becomes even less informative with nonlinear transfers, where changes in the force constants of the bending vibrations have to be considered and where there are significant changes in solvation on the route to the activated complex. To that extent, it appears that the KSIE can be regarded as a secondary solvent effect because, in the course of the reaction, solvation of O1 by water is replaced by intramolecular hydrogen-bonding that involves the imidazolium moiety. Little is to be gained by the discussion of small changes in KSIE values that are secondary and are close to unity. Literature values are consistent with this analysis, and as expected, the KSIE for the hydrolysis of a 4-nitrophenyl phosphate monoanion is ca. 0.96.[24] In addition, the activation parameters estimated in the pH-independent region (Figure 2), at pH 2.48, 3.00, and 3.29, are $\Delta H^{\ddagger} = 28.2 \pm 0.1$ kcal/mol and $\Delta S^{\ddagger} = +2.0 \pm 0.3$ e.u. This shows an entropy term that is very similar to those of other phosphate monoester monoanion hydrolyses, which are ranged between −1 and −6 e.u.[12] Finally, according to the phosphate monoester monoanion hydrolyses correlation as follows,

$$\log k_2 = -0.87 - 0.27 \mathrm{p}K_{\mathrm{LG}} \qquad (4)$$

in s^{-1} at 100 °C,[12] a pK_{LG} of 8.5 could be calculated, which is similar to that reported for the hydrolysis of 2-(4-(5)-imidazolyl)-phenyl phosphate.[25] The pK_{LG} value calculated in aqueous solution must be different from that obtained through the bondlength correlations because the conformation of the phosphate moiety in solid and in solution differs.

Computational Studies. Full, unconstrained geometry optimization and frequency calculations of the species $IMPP^+$, $IMPP^{\pm}$, and $IMPP^-$ were performed at the density functional theory (DFT) level, with the B3LYP hybrid density functional.[26,27] The 6-31G(d) basis set[28] was used for the H, C, N, O, and P atoms, with the explicit inclusion of diffuse and *p* polarization functions[29] on O, N, and H. The structures were optimized in aqueous solution, within the PCM dielectric continuum approach.[30] For each species investigated, two stable structures were obtained through rotation around the C1−C11 bond. The structures labeled as conformers ***a*** have the imidazolium group out of the plane that is formed by the benzene ring, which favors hydrogen-bond formation between the NH group of the imidazolium group and O4. In the structures that correspond to the conformers labeled as ***b*** the two rings are almost coplanar, which favors hydrogen-bond formation between the NH and O1. Figure 5 shows the main structural parameters that were computed for the structures ***a*** and ***b*** of

(24) Grzyska, P. K.; Czyryca, P. G.; Purcell, J.; Hengge, A. C. *J. Am. Chem. Soc.* **2003**, *125*, 13106−13111.
(25) Benkovic, S. J.; Dunikoski, L. K. Jr., *J. Am. Chem. Soc.* **1971**, *93*, 1526−1527.
(26) Becke, A. D. *J. Chem. Phys.* **1993**, *98*, 5648−5652.
(27) Lee, C.; Yang, W.; Parr, R. G. *Phys. Rev. B* **1998**, *37*, 785−789.
(28) Ditchfield, R.; Hehre, W. J.; Pople, J. A. *J. Chem. Phys.* **1971**, *54*, 724.
(29) Hehre, W. J.; Ditchfield, R.; Pople, J. A. *J. Chem. Phys.* **1972**, *56*, 2257.
(30) Cossi, M.; Barone, V.; Cammi, R.; Tomasi, J. *Chem. Phys. Lett.* **1996**, *255*, 327.

$IMPP^+$, $IMPP^{\pm}$, and $IMPP^-$, as well as the relative energies, ΔE ($E_b - E_a$), between them.

Hydrogen-bonding between the NH and O4 appears to generate conformers that are more stable than those generated by hydrogen-bonding between NH and O1. The P1−O1 bond length, in conformers ***b***, decreases, following the order $IMPP^-$ > $IMPP^{\pm}$ > $IMPP^+$, and is likely the result of the favored hydrogen-bond between NH and O1. The degree of ionization of the phosphate group also determines the degree of the proton-transfer and lengthening of the P1−O1 bond. An increase of 0.05 Å, from conformer ***a*** to ***b*** in $IMPP^-$, results from a hydrogen-bond that is 0.456 Å shorter in conformer ***b***. The influence of electronic effects of substituents on the imidazolium group is very high. The imidazolium group exhibits a Hammett ρ of ca. 11,[31] and with this magnitude of the Hammett similarity constant, simple protonation of the phosphate group favors proton-transfer.

Because kinetic effects are strongly dependent on the conformational equilibrium between ***a*** and ***b***, it is important to note that in $IMPP^-$ the less reactive conformer ***a*** is 9.3 kcal·mol^{-1} more stable, which slows the reaction. Conversely, in $IMPP^+$ the difference is so small (1.2 kcal·mol^{-1}) that it is in the range of energy contribution from thermal energy. Thus, the freedom of both imidazole and phosphate groups and the magnitude of ΔE between conformers ***a*** (less reactive) and ***b*** (most reactive conformer) are determinant factors for proton-transfer from the general acid. The rate enhancement and differences in energy between the conformers follow the order $IMPP^+$ > $IMPP^{\pm}$ > $IMPP^-$. As generally observed for organic compounds where rotational freedom is present, the small energy differences between a variety of conformers result in a flat potential energy surface (PES).[32] As a consequence of the very nature of the energy surface, some of the structures obtained in Figure 5 are not true energy minima on the PES, which shows a small negative eigenvalue on the Hessian matrices. However, because of the large energy differences, the qualitative trends obtained by these results are not affected, and the reported calculations for isolated molecules are consistent with the involvement of an intramolecular proton-transfer in the course of the reaction. Work is in progress to quantitatively describe, by using a combined quantum mechanics/molecular mechanics (QM/MM) technique, proton-transfer reactions in enzyme models.

Conclusions

The data on IMPP hydrolysis indicate that in water there is no significant acceleration by the imidazolium moiety whose effect disappears in going from $IMPP^+$ to $IMPP^-$ and $IMPP^{2-}$, where hydrolyses are very slow. This conclusion indicates that the rate enhancement depends on intramolecular hydrogen-bonding with the O1 rather than with the phosphoryl oxygen O4. The near-planar conformation of the imidazolium and phenyl groups in the activated complex, as in the naphthyl derivative, **1**, is particularly important in considering models for enzymatic reactions and should be relevant in the design of new models. The presence of a relatively free NH in the imidazolium (N2 atom), which can hydrogen-bond to water, probably decreases the intramolecular catalytic efficiency relative to that in **1**.

(31) Charton, M. *J. Org. Chem.* **1965**, *30*, 3346−3350.
(32) Florián, J.; Warshel, A. *J. Phys. Chem. B* **1998**, *102*, 719.

Experimental Section

Materials. Inorganic salts were of analytical grade and were used without further purification. Liquid reagents were purified by distillation. 2-(2′-Hydroxyphenyl)imidazole was prepared by the method of Rogers and Bruice.[33]

Synthesis of IMPP. A solution of PCl_5 (650 mg, 3.12 mmol) in $CHCl_3$ (15 mL) was added dropwise to a $CHCl_3$ solution of 2-(2′-hydroxyphenyl)imidazole (500 mg, 3.12 mmol in 15 mL) in an ice−water bath. The mixture was stirred at room temperature for 60 min. Water was then added (0.25 mL), and the mixture was left to react overnight. The solvent was removed under reduced pressure, and acetone (20 mL) and water (5 mL) were added to the resulting crude oil. White, fine crystals were immediately obtained and were collected by filtration. Purification was carried out by dissolving the crude product in water (30 mL), at pH 7.8 (NaOH), and unreacted phenol was extracted with $CHCl_3$ (3 × 10 mL). The resulting water layer was concentrated in vacuo (<40 °C) to 5 mL. The pH was adjusted to 4.5 with HCl, and methanol (3 mL) was added. White crystals of NaCl were filtered off. Colorless lapidated, diamond-like crystals of the product were obtained by slow evaporation of the solvent at room temperature. Alternatively, methanol was added directly to the concentrated solution at pH 7.8 to give the sodium salt of IMPP. mp. 222−224 °C (dec) zwitterionic form. NMR measurements were carried out at pD = 6.25 (monoanionic form): ^{31}P NMR (81 MHz, D_2O, external reference H_3PO_4 85%) δ −1.10 ppm, s; ^{13}C NMR (100 MHz, D_2O, internal reference TSP) δ 117.9, 122.0, 125.8, 126.5, 131.4, 136.2, 144.5, 154.0; ^{1}H NMR (400 MHz, D_2O, internal reference TSP) δ 7.26 (ddd, 1H, J = 7.5, 7.5, and 3.4 Hz), 7.46 (d, 2H), 7.53 (dd, 1H, J = 8.0 and 3.5 Hz), 7.57 (m, 1H), 7.70 (dd, 1H, J = 7.8 and 2.8 Hz).

pK_a Determination. Potentiometry. The pK_a of IMPP was determined with a digital pH meter and a combined glass electrode. Titrations were performed in a 150 mL thermostated cell, under N_2 at 25.0 °C, an ionic strength of 0.1 M KCl, and the initial [IMPP] was 1.0 mM. The solution was titrated with small increments of 0.1008 M KOH, which was CO_2 free. All precautions were taken to eliminate carbonate and CO_2 during the titration. The value of pK_w was taken as −13.78. The program BEST7[34] was used to calculate the dissociation constants.

Spectrophotometric pH Titration. Absorbance measurements were made over a pH range with 66.7 μM of IMPP on a diode-array spectrophotometer with a thermostated cell holder at 25.0 °C. Solutions were buffered with (0.01 M of each) HCOOH (pH 3−4.5), CH_3COOH (pH 4−5.5), NaH_2PO_4 (pH 5.5−7.8), and H_3BO_3 (pH 7.8−9.0).

^{31}P NMR Titration was performed at 81 MHz and 25.0 °C. Chemical shifts were measured in D_2O with H_3PO_4 85% as an external reference. The IMPP solution (10 mg/mL) was first adjusted to pH 9.3 with NaOD and then titrated by return with DCl until pH 4.6 was reached, where IMPP starts to precipitate. The value of pD was corrected with $pD = pH_{read} + 0.4$.[35]

Kinetics. Hydrolyses of IMPP were followed spectrophotometrically by monitoring the appearance of 2-(2′-hydroxyphenyl)-imidazole at 310 nm. The temperatures of reaction solutions in quartz cuvettes were controlled with a thermostated water-jacketed cell holder. Ionic strengths were 1.0 M with KCl. The reaction was initiated by the injection of 20 μL of 10 mM stock solutions of IMPP in water (at pH ∼ 10 and stored in a refrigerator to minimize hydrolysis) into 3 mL of aqueous solutions to give 66.7 μM IMPP. Absorbance versus time data were stored directly on a microcom-

(33) Rogers, G. A.; Bruice, T. C. *J. Am. Chem. Soc.* **1974**, *96*, 2463−2472.
(34) Martell, A. E.; Smith, Z. M.; Motekaitis, R. J. *NIST Critical Stability Constants of Metal Complexes Database: NIST Standard Reference Database 46*; NIST: Gaithersburg, MD, 1993.
(35) Schowen, K. B. J. In *Transition States of Biochemical Processes*; Gandour, R. D., Ed.; Plenum: New York, 1978; pp 225−284.

puter, and first-order rate constants, k_{obs}, were calculated from linear plots of $\ln(A_\infty - A_t)$ against time for at least 90% of the reaction by using an iterative least-squares program; correlation coefficients were >0.999 for all kinetic runs. The pH was maintained with 0.01 M buffers of $CH_2ClCOOH$ (pH 2−3), HCOOH (pH 3−4.5), CH_3COOH (pH 4−5.5), and NaH_2PO_4 (pH 5.5−6.0). In solutions where [HCl] > 0.01 M, the reactions were self-buffered with no correction for ionic strength.

X-ray Crystallography. The crystal data were measured on an Enraf−Nonius CAD4 diffractometer, with graphite monochromated Mo−K_α radiation ($\lambda = 0.71069$ Å) and at room temperature. Cell parameters were determined from 25 carefully centered reflections in the θ range 6.85−18.41° and were refined by the least-squares method. The ω-2θ scan technique for an orthorhombic system was used to collect 2667 reflections, which represents 1/8 of the Ewald sphere. Intensity was controlled by the use of three standard reflections, which were measured at regular intervals, and no significant loss of intensity was observed during the data collection. The collected intensities were corrected for Lorentz and for polarization effects.[36] The structure was solved by direct methods and was refined by the full-matrix least-squares method using the SIR97[37] and the SHELXL97[38] computer programs, respectively. The absolute structure was not determined by the X-ray analysis. All non-hydrogen atoms were refined with anisotropic displacement parameters. Hydrogen atoms were placed at idealized positions by using standard geometric criteria. The molecular structure was drawn with the ORTEP3 program.[39] Selected crystallographic data: formula $C_9H_9N_2O_4P$, FW 240.15; crystal system: hexagonal; space group: $P6_5$ (No. 170), $a = 9.0850(9)$ Å, $c = 20.973(3)$ Å, $\gamma = 120°$, $V = 1499.2(3)$ Å^3, $Z = 6$, $\rho_{calc} = 1.596$ Mg/m^3, $\mu = 0.275$ mm^{-1}, F(000) = 744; 2667 reflections collected, 1228 unique ($R_{int} = 0.0291$); Full-matrix least-squares on F^2, 148 refined parameters, GOF (F^2) 1.041, R_1 [$I > 2\sigma(I)$] = 0.0289 and wR_2 (all data) = 0.0726.

Computations. DFT calculations were carried out by using the Gaussian 03 program[40] that employed the hybrid B3LYP functional. Geometry optimizations were taken in the water dielectric continuum as implemented in the PCM model. The 6-31G* basis set was used for all atoms, with explicitly diffuse and *p* polarization functions on O, N, and H atoms.

Acknowledgment. We are indebted to PRONEX, FINEP, CNPq, and the National Science Foundation for financial support of this work.

Supporting Information Available: Potentiometric titration of IMPP, proton inventory, rate constants as a function of temperature, CIF file deposited in CSD (No. 630873), selected geometric parameters for structures used in the bond length-reactivity correlations, and an attempt to survey over CSD and Cartesian coordinates of the B3LYP optimized structures. This material is available free of charge via the Internet at http://pubs.acs.org.

JO070090R

(36) Spek, A. L. *HELENA: CAD-4 Data Reduction Program*; University of Utrecht: The Netherlands, 1996.

(37) Altomare, A.; Burla, M. C.; Camalli, M.; Cascarano, G.; Giacovazzo, C.; Guagliardi, A.; Moliterni, A. G. G.; Polidori, G.; Spagna, R. *J. Appl. Crystallogr.* **1999**, *32*, 115−119.

(38) Sheldrick, G. M. *SHELXL97: Program for the Refinement of Crystal Structures*; University of Göttingen: Germany, 1997.

(39) Farrugia, L. J. *J. Appl. Crystallogr.* **1997**, *30*, 565.

(40) Frisch, M. J.; Trucks, G. W.; Schlegel, H. B.; Scuseria, G. E.; Robb, M. A.; Cheeseman, J. R.; J. A. Montgomery, J.; Vreven, T.; Kudin, K. N.; Burant, J. C.; Millam, J. M.; Iyengar, S. S.; Tomasi, J.; Barone, V.; Mennucci, B.; Cossi, M.; Scalmani, G.; Rega, N.; Petersson, G. A.; Nakatsuji, H.; Hada, M.; Ehara, M.; Toyota, K.; Fukuda, R.; Hasegawa, J.; Ishida, M.; Nakajima, T.; Honda, Y.; Kitao, O.; Nakai, H.; Klene, M.; Li, X.; Knox, J. E.; Hratchian, H. P.; Cross, J. B.; Adamo, C.; Jaramillo, J.; Gomperts, R.; Stratmann, R. E.; Yazyev, O.; Austin, A. J.; Cammi, R.; Pomelli, C.; Ochterski, J. W.; Ayala, P. Y.; Morokuma, K.; Voth, G. A.; Salvador, P.; Dannenberg, J. J.; Zakrzewski, V. G.; Dapprich, S.; Daniels, A. D.; Strain, M. C.; Farkas, O.; Malick, D. K.; Rabuck, A. D.; Raghavachari, K.; Foresman, J. B.; Ortiz, J. V.; Cui, Q.; Baboul, A. G.; Clifford, S.; Cioslowski, J.; Stefanov, B. B.; Liu, G.; Liashenko, A.; Piskorz, P.; Komaromi, I.; Martin, R. L.; Fox, D. J.; Keith, T.; Al-Laham, M. A.; Peng, C. Y.; Nanayakkara, A.; Challacombe, M.; Gill, P. M. W.; Johnson, B.; Chen, W.; Wong, M. W.; Gonzalez, C.; Pople, J. A.; Gaussian Inc.: Wallingford, CT, 2004.